Food Hydrocolloids 152 (2024) 109951

Contents lists available at ScienceDirect

Food Hydrocolloids

journal homepage: www.elsevier.com/locate/foodhyd

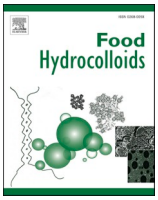

Closing the loop: Waste valorisation from vegetal sources to develop fruit active films

Jone Uranga [a], Itsaso Leceta [a], Pedro Guerrero [a,b,**], Koro de la Caba [a,b,*]

[a] BIOMAT Research Group, University of the Basque Country (UPV/EHU), Escuela de Ingeniería de Gipuzkoa, Europa Plaza 1, 20018, Donostia-San Sebastián, Spain
[b] BCMaterials, Basque Center for Materials, Applications and Nanostructures, UPV/EHU Science Park, 48940, Leioa, Spain

ARTICLE INFO

Keywords:
Bio-waste
Valorization
Circular economy
Active films

ABSTRACT

Cellulose-rich residue after agar extraction was incorporated into gelatin film forming formulations in order to revalorize it and improve film properties. This revalorized cellulose was compared with the commercial sodium carboxymethyl cellulose, also employed in gelatin films. Cellulose addition improved water resistance and UV light barrier properties of films, contributing to food shelf life extension. Additionally, grape marc extract was incorporated into cellulose-containing gelatin film forming formulations to promote antioxidant activity. These films showed the ability to be thermo-sealed and were used to pack grapes, thus, closing the loop from food waste to food packaging.

1. Introduction

Market growth, excessive plastic production, unlimited waste generation, disposal challenges and eco-friendly materials demand have stimulated research to produce bio-based packaging as an alternative to conventional petroleum-based packaging (Chen et al., 2022; Zhang et al., 2023). In this context, the food industry generates a large amount of biodegradable by-products, which can be used to extract biopolymers (Usman et al., 2023). In particular, during the production and processing of food, bones and skins are discarded and can be valorized to obtain collagen and gelatin through collagen denaturation. Gelatin consists of a mixture of single and double unfolded chains of hydrophilic character and is considered a promising biopolymer owing to its abundance, non-toxicity, biocompatibility, good film-forming ability, transparency and potential use as a carrier of different compounds (Toniciolli Rigueto et al., 2022; Alipal et al., 2021).

Modification of native gelatin with suitable additives is needed to enhance mechanical, water and thermal stability and, thus, improve the functional properties of gelatin films (Liu et al., 2022). In this regard, the combination of gelatin with different biopolymers can be another strategy to overcome the gelatin shortcomings. Many studies have been conducted on cellulose- or cellulose derivative-containing gelatin films. For instance, Salimiraad et al. (2022) prepared gelatin/nanocellulose/nanochitosan films for the preservation of chicken fillets. Azarifar et al. (2020) utilized gelatin/carboxymethylcellulose films and Nguyen et al. (2023) used gelatin/carboxymethylcellulose/guar gum films for the preservation of raw beef. Moreover, cherry tomatoes were preserved with gelatin/carboxymethylcellulose films by Samsi et al. (2019). Regarding the use of cellulose to develop films (Rachtanapun et al., 2012) or as reinforcement for other biopolymers (Uranga et al., 2023), this polysaccharide can be extracted from waste to promote a environmentaly friendlier approach.

Larger tannin structures, flavonols and polymeric pigments present in agro-food-industry by-products have also shown binding affinity to proteins as well as significant antioxidant and antimicrobial activity (Etxabide et al., 2022). Employing them may therefore be beneficial for providing interactions and structural modifications in gelatin films on top of preparing active packaging materials designed to extend the shelf-life of packaged foods by including antioxidant/antimicrobial compounds (Luo et al., 2022). Recovering phenolics from agro-food industry by-products and adding them to gelatin formulations may enhance the functional properties of the resulting films (Gil-Martín et al., 2022). In this context, winemaking main residues obtained after the pressing step, known as grape pomace or grape marc, comprised of

* Corresponding author. BIOMAT Research Group, University of the Basque Country (UPV/EHU), Escuela de Ingeniería de Gipuzkoa, Europa Plaza 1, 20018, Donostia-San Sebastián, Spain.
** Corresponding author. BIOMAT Research Group, University of the Basque Country (UPV/EHU), Escuela de Ingeniería de Gipuzkoa, Europa Plaza 1, 20018, Donostia-San Sebastián, Spain.
E-mail addresses: pedromanuel.guerrero@ehu.es (P. Guerrero), koro.delacaba@ehu.es (K. de la Caba).

https://doi.org/10.1016/j.foodhyd.2024.109951
Received 5 January 2024; Received in revised form 25 February 2024; Accepted 26 February 2024
Available online 27 February 2024

grape stems, seeds and skins, can be mentioned as sources of structurally diverse phenolic compounds (Jelley et al., 2020).

This work reports the manufacturing of gelatin-based films with cellulose from different sources, comparing the results obtained with commercial sodium carboxymethyl cellulose or cellulose form agar production residue. Moreover, this work aims to determine whether the grape marc extract could be an appropriate antioxidant for developing active packaging films. Finally, the potential of gelatin films to improve the shelf-life of grapes was explored.

2. Materials and methods

2.1. Materials

Commercial porcine gelatin (type A, 270 bloom) (Sancho de Borja, Spain), anhydrous citric acid (Panreac, Spain), agar production residue, containing mostly cellulose and designated as AR (Roko agar, Spain), sodium carboxymethyl cellulose, designated as SCMC (Mw ≈ 250,000, degree of substitution 0.7) (Sigma-Aldrich, USA), and glycerol (Panreac, Spain) were used in film forming formulations. Moreover, red grape marc extracted with water (Zujovic et al., 2021) and obtained from the Auckland region was kindly supplied by the School of Chemical Sciences of the University of Auckland (Auckland, New Zealand). This extract was designated as GME. All chemicals were used as received without further purification.

2.2. Preparation of films

Gelatin films were prepared by mixing gelatin, citric acid and AR or SCMC in distilled water. The citric acid content employed in this work was 20 wt % (on gelatin dry basis) and the AR or SCMC contents employed were 0, 10 or 20 wt % (on gelatin dry basis). Solutions were heated at 80 °C for 30 min and stirred at 200 rpm. Then, 20 or 30 wt % glycerol (on gelatin dry basis) was added as a plasticizer and the solution pH was adjusted to 7 with NaOH (1 M). The heating procedure at 80 °C was repeated for other 30 min at 200 rpm and finally, solutions (~27 g) were poured into Petri dishes and allowed to dry for 48 h at room temperature. Films with 20 wt % glycerol were designated as 20Control, 20Gly10SCMC, 20Gly20SCMC, 20Gly10AR, and 20Gly20AR, as a function of the SCMC or AR content. Similarly, films with 30 wt % glycerol were designated as 30Control, 30Gly10SCMC, 30Gly20SCMC, 30Gly10AR, and 30Gly20AR. Moreover, films containing GME were prepared adding 1 or 2 wt % GME (on gelatin dry basis) before the pH modification step. Specifically, GME was added into 30Gly20SCMC and the resulting films were designated as SCMC1GME, SCMC2GME as a function of GME content, and GME was added into 30Gly20AR and the resulting films were designated as AR1GME and AR2GME as a function of GME content.

2.3. Characterization of films

2.3.1. Scanning electron microscopy (SEM)

The morphology of films was visualized using an S-4800 field emission scanning electron microscope (Hitachi High-Technologies Corporation). Prior to observation, samples were mounted on a metal stub with double-sided adhesive tape and coated under vacuum with gold (JFC-1100) in an argon atmosphere. Films were analysed employing an accelerating voltage of 5 kV.

2.3.2. X-ray diffraction (XRD)

XRD study was carried out using an Xpert PRO diffraction unit (PANalytical). The radiation was generated from a CuKα (λ = 1.5418 Å) source (40 mA, 40 kV). Data were collected from 2θ values from 2 to 50°, where θ is the incidence angle of the X-ray beam on the films.

2.3.3. Fourier transform infrared (FTIR) spectroscopy

FTIR spectra of films were achieved on a Platinum-ATR Alpha II FTIR spectrometer (Bruker). A total of 32 scans were performed at a resolution of 4 cm^{-1} in the wavenumber range from 800 to 4000 cm^{-1}.

2.3.4. Swelling measurements

In order to calculate the swelling capacity of films, different pre-weighed (w_p) samples were immersed into 40 mL of water at room temperature and then weighed again at various time points (w_t) until constant values were obtained. The swelling (S) was calculated using Equation (1):

$$S\ (\%) = \frac{w_t - w_p}{w_p} \cdot 100 \quad (1)$$

2.3.5. Total soluble matter (TSM)

In order to determine the weight loss due to the hydrolytic effect, films were weighed (w_p) and subsequently immersed into water (40 mL) at room temperature. After 24 h, samples were removed and dried in the oven at 105 °C for 24 h and reweighed (w_{1d}). To calculate the hydrolytic degradation Equation (2) was used:

$$TSM\ (\%) = \frac{w_p - w_{1d}}{w_p} \cdot 100 \quad (2)$$

2.3.6. Moisture content (MC)

To determine the MC of films, specimens were weighed (w_0) and then dried in an oven at 105 °C for 24 h. After this time, samples were reweighed (w_1) to determine their MC using Equation (3):

$$MC\ (\%) = \frac{w_0 - w_1}{w_0} \cdot 100 \quad (3)$$

2.3.7. Water vapour transmission rate (WVTR)

WVP values were measured in a controlled humidity environment chamber PERME™ W3/0120 (Labthink Instruments Co. Ltd.). Film disks (Ø = 7.4 cm) were sealed to cups containing distilled water. Then, cups were placed into the chamber at 38 °C and 90% relative humidity, according to ASTM E96-00. WVTR was determined gravimetrically using Equation (4):

$$WVTR\left(\frac{g}{m^2 \bullet day}\right) = \frac{\Delta w}{A \cdot \Delta t} \quad (4)$$

where A is the exposed area of the film (m^2), Δw is the mass of the absorbed water (g) during time, and Δt is 1 day.

2.3.8. UV resistance

Light absorption was measured in the UV–vis range (200–800 nm) using a UV Multiskan SkyHigh ultraviolet–visible (UV–Vis) spectrophotometer (Thermo Scientific).

2.3.9. Colour and gloss

Colour parameters (L*, a*, b*) were determined using a CR-400 Minolta Chroma-Meter colourimeter (Konica Minolta). Films were placed on the surface of a white standard plate (calibration plate values: L* = 97.39, a* = 0.03 and b* = 1.77) and colour parameters were measured using the CIELAB colour scale: L* = 0 (black) to L* = 100 (white), -a* (greenness) to +a* (redness), and -b* (blueness) to + b* (yellowness). Total colour difference (ΔE*) was calculated referred to the 20Control or 30Control specimens using Equation (5):

$$\Delta E^* = \sqrt{(\Delta L^*)^2 + (\Delta a^*)^2 + (\Delta b^*)^2} \quad (5)$$

2.3.10. Differential scanning calorimetry (DSC)

DSC was carried out in a Mettler Toledo DSC 822 (Mettler Toledo S. A.E.). Samples (3.0 ± 0.2 mg) were sealed in aluminium pans to avoid mass loss during the experiment. Filled pans were heated from −50 to

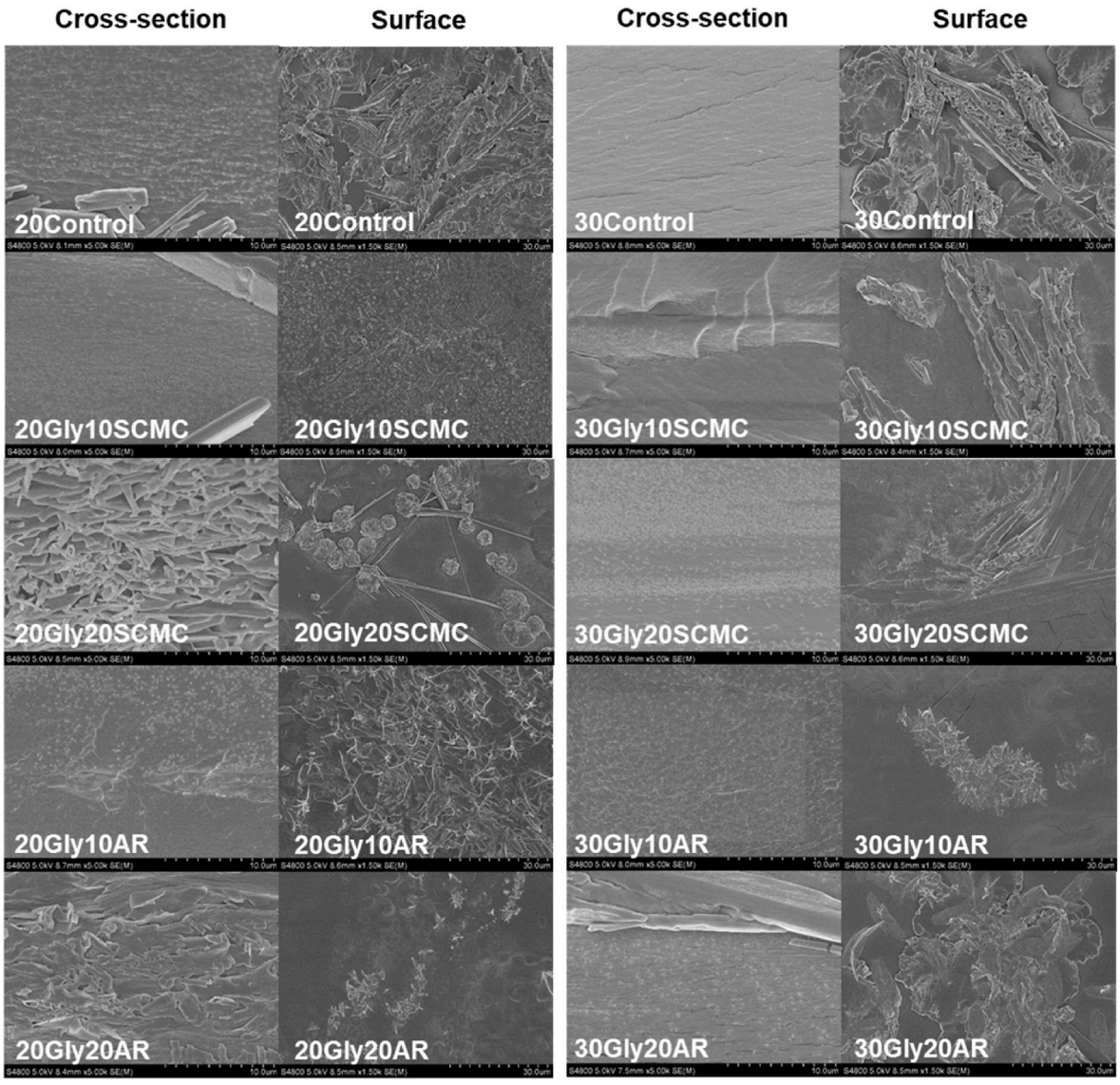

Fig. 1. Cross-sectional and surface SEM images for the films.

250 °C at a rate of 10 °C/min under inert atmosphere conditions to avoid thermo-oxidative reactions.

2.3.11. Tensile test

TA.XT.Plus C Texture Analyzer (Aname), with a 5 kg load cell, was used to carry out tensile tests at 1 mm/s. Samples with 22.25 mm length and 4.75 mm width were used and conditioned in a controlled chamber at room temperature and 100% relative humidity before testing.

2.4. Characterization of GME

2.4.1. pH sensitivity

Solutions with different pH (1-14) were prepared with diluted HCl and NaOH. 1 mg GME was dissolved in 10 mL of the abovementioned solutions. The colour of the solution was observed and photographed. Then the solution under various pH conditions was scanned at wavelengths ranging from 200 to 800 nm and the changes in the absorption wavelength were recorded (Wang et al., 2022).

2.5. Characterization of extract-containing films

2.5.1. Extract release and DPPH radical scavenging activity

First, the calibration line for GME (0.005–0.04 mg/mL) was determined: $y = 0.0004 + 10.046x$ ($R^2 = 0.999$). The wavelength used for the calibration was 277 nm due to the predominant presence of anthocyanins in GME. Then, the GME release was calculated by the immersion of films (1 cm × 2 cm) into a 20% ethanol solution (10 mL) at room temperature for 2 days. According to the Commission Regulation No 10/2011 (EU, 2011), 20% ethanol solution was employed considering that the films prepared in this work could be appropriate to package fruit in its own juice, more specifically, peeled grapes. Samples were immersed into dark glass vessels to protect the bioactive compounds from light. A spectrophotometer was employed to measure the light absorption from 200 to 800 nm. The absorption spectra of the solutions were recorded at 30, 90, 180, and 300 min and then, every 24 h up to 2 days.

DPPH radical scavenging activity was measured for GME-containing films (1 cm × 1 cm into 10 mL 20% ethanol solution). Briefly, 2 mL of GME-released solution was mixed with 2 mL of DPPH solution (75 mM in methanol). The mixture was vigorously shaken and then, allowed to stand at room temperature in the dark for 30 min. The inhibition values (I) were determined by the absorbance decrease at 517 nm using

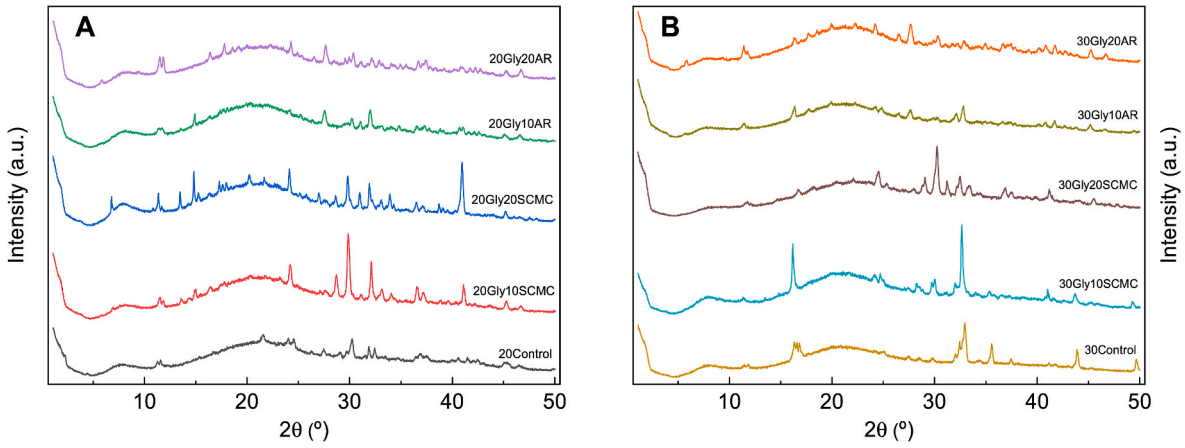

Fig. 2. XRD patterns of SCMC- or AR-containing gelatin films with (A) 20 wt % and (B) 30 wt % glycerol.

Equation (6):

$$I\ (\%) = \frac{A_c - A_{sample}}{A_c} \cdot 100 \quad (6)$$

where A_c is the absorbance of the DPPH solution and A_{sample} is the absorbance of the DPPH solution with GME.

2.5.2. Application of films in the conservation of grapes

To determine the performance of the films in peeled grapes preservation, Vargas-Torrico et al. (2022) method with some modifications was employed. Red grapes were purchased from a local market, peeled, sealed in between the films and kept in the fridge at 4 °C. Photographs were taken with a Tough TG-6 (Olympus) high-resolution camera every 24 h for 7 days. Moreover, since increasing sugar concentration and decreasing titratable acidity occur in the ripening processes and these are indicators of consumer acceptability (Jayasena, 2008), pH and Brix value changes were recorded employing a HI981032 foodcare pH Tester (Hanna Instruments) and a HI 96800 digital refractometer for refractive index and Brix measurements (Hanna Instruments). Moreover, the colour change was also analysed with a CR-400 Minolta Chroma-Meter colourimeter (Konica Minolta).

2.6. Statistical analysis

Analysis of variance (ANOVA) was used to determine the significance of differences among samples. The analysis was performed with an SPSS computer program (SPSS Statistic 28.0) and Tukey's test was used for multiple comparisons. Differences were statistically significant at the $p < 0.05$ level. The analysis was carried out separately for the systems with 20 and 30 wt % glycerol in order to estimate the significant differences as a function of SCMC and AR. In the case of GME-containing films, the analysis was carried out separately for the systems with SCMC and AR in order to estimate the significant differences as a function of GME content.

3. Results and discussion

3.1. Characterization of films without GME

3.1.1. Morphological and structural characterization

SEM images of the film cross-section and surface can be seen in Fig. 1. Even if samples exhibited crack-free compact cross-sections, the microstructures of 20Gly20SCMC (C.1) and 20Gly20AR (E.1) displayed a more noticeable fibrous web-like structure, related to the fibrous character of cellulose (Hassan et al., 2020) highly present in these formulations. The same content of cellulose with higher glycerol content did not lead to visible fibrous structures (30Gly20SCMC (H.1) and 30Gly20AR (J.1)) due to a bigger internal space between polymer chains that could ease the orientation of cellulose fibrous structures (Guo et al., 2022). In a similar manner to the cross-section, fibres were hardly found in the surfaces of films with 30 wt % of glycerol (G.2, H.2, I.2, J.2), whereas 20 wt % glycerol-containing films (B.2, C.2, D.2, E.2) showed a higher fibre content on the surface. Otherwise, rough surfaces could be observed in SEM images.

XRD patterns of films are shown in Fig. 2. All films exhibited the

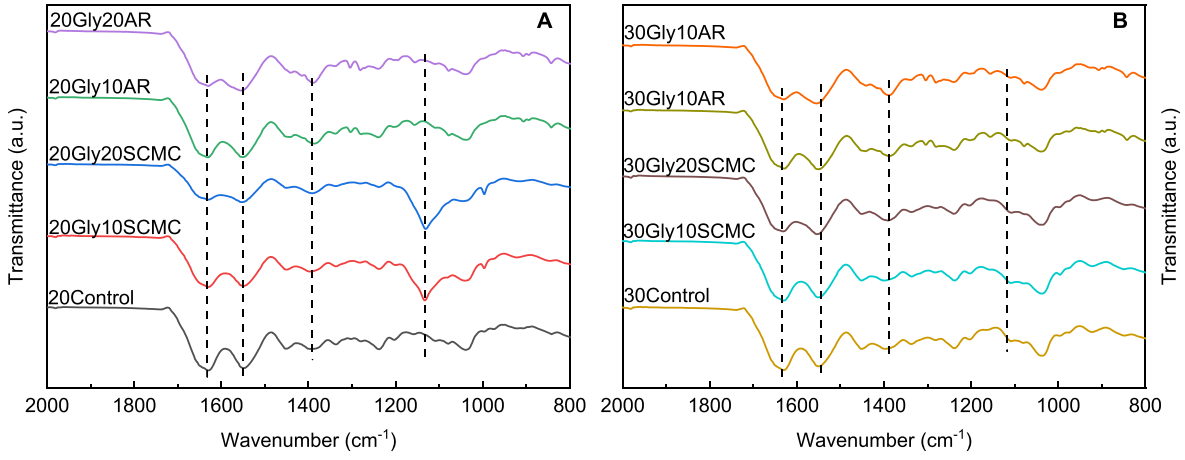

Fig. 3. FTIR spectra of SCMC- or AR-containing gelatin films with (A) 20 wt % and (B) 30 wt % glycerol from 2000 to 800 cm^{-1}.

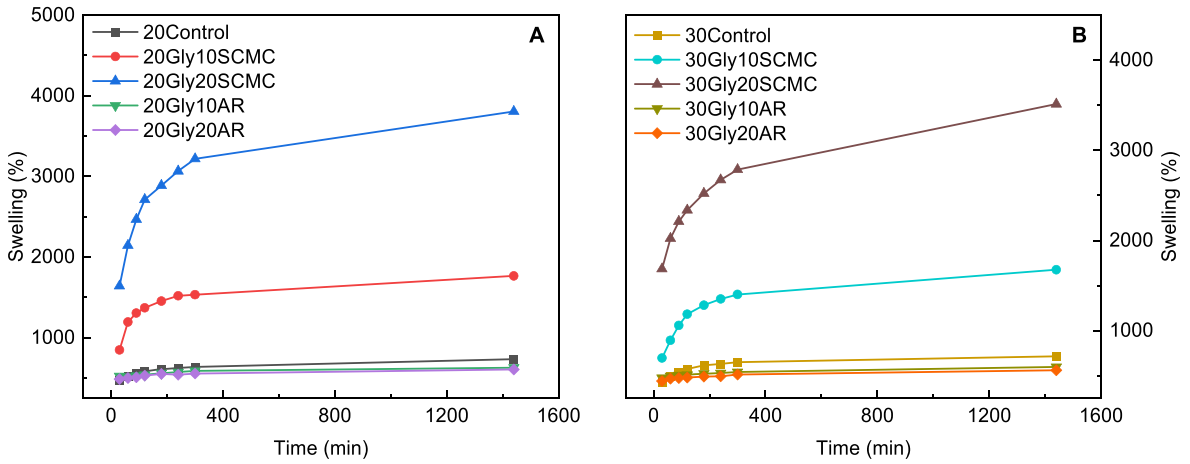

Fig. 4. Swelling behaviour of SCMC- or AR-containing gelatin films with (A) 20 wt % and (B) 30 wt % glycerol.

characteristic gelatin XRD pattern, which includes two reflection peaks at 8 and 21°. The first peak is related to the diameter of the residual triple-helix from native collagen and the second peak is associated with the partial crystalline structure of gelatin (Liu et al., 2015). Moreover, the presence of cellulose, which is semi-crystalline in nature, influenced these X-ray patterns. In fact, native cellulose exhibited three characteristic peaks around 14, 22 and 33° (Mondal et al., 2015), while SCMC showed a broad diffraction peak around 18-27° (Li et al., 2020), owing to the destruction of the crystalline structure of the original cellulose. Otherwise, films showed sharp diffraction peaks (14, 17, 24, 29, 31, 34, 37, 41, 43°), since citric acid has small molecular and strong crystal diffractions (Diop et al., 2023). These crystal peaks related to pure citric acid were fewer for 30 wt % glycerol-containing films and AR-containing films, indicating that the citric acid was better dispersed in the films with those compositions (Shi et al., 2007).

3.1.2. Physicochemical properties

FTIR spectroscopy was used to examine the interactions between the film components and spectra are presented in Fig. 3. The broad band above 3000 cm^{-1}, observed in all spectra, corresponded to the hydroxyl (-OH) and amino (-NH) groups (Figure S1). Even if citric acid was present in all film formulations, there was no presence of the two characteristic bands of citric acid around 1700 cm^{-1} and 1750 cm^{-1} associated with C═O stretching bands (Ludmerczki et al., 2019). Based on our previous study (Uranga et al., 2016), this fact together with the presence of a peak related to carbonyl groups around 1630 cm^{-1} suggested that cross-linking occurred between gelatin and citric acid. On top of that, the relative intensity between the amide I (≈1630 cm^{-1}) and amide II (≈1552 cm^{-1}) bands of gelatin changed. In particular, the relative intensity of the band corresponding to the amide I was higher for control and 10 wt % SCMC-containing films, 20Gly10AR and 30Gly10AR showed similar relative intensity of amide I and II, meanwhile the relative intensity of the band corresponding to the amide I was lower for the 20Gly20SCMC, 20Gly20AR, 30Gly20SCMC and 30Gly20AR films. The amide I band intensity is dependent on the protein chain conformation (Andonegi et al., 2020), thus, these results revealed that the high structural order related to the triple-helical structure is slightly modified in films. Moreover, the intensity of the band at 1390 cm^{-1}, related to hydrogen-bonded COO- groups (Xiao et al., 2014), was higher in films with AR. Overall, these results might indicate that physicochemical interactions were noticeable in films and more likely to happen in films with AR. On the other hand, the glycerol content difference had a strong influence in SCMC-containing films and the most noticeable change occurred in the band at 1132 cm^{-1}, associated with sugar ring vibrations (Dharmalingam & Anandalakshmi, 2019), disappearing when glycerol content was 30 wt %.

Table 1
Moisture content (MC) and total soluble matter (TSM) values of SCMC- or AR-containing gelatin films with 20 wt % and 30 wt % glycerol.

Film	TSM (%)	MC (%)
20Control	38.3 ± 7.6^{a}	15.2 ± 0.6^{ab}
20Gly10SCMC	34.8 ± 2.2^{ab}	17.3 ± 0.7^{c}
20Gly20SCMC	28.9 ± 1.1^{ab}	16.4 ± 0.2^{bc}
20Gly10AR	27.9 ± 0.6^{b}	14.9 ± 0.2^{a}
20Gly20AR	26.6 ± 0.9^{b}	15.2 ± 0.6^{ab}
30Control	37.1 ± 1.4^{a}	16.2 ± 0.9^{a}
30Gly10SCMC	32.7 ± 0.5^{ab}	16.3 ± 0.2^{a}
30Gly20SCMC	30.2 ± 3.3^{b}	14.5 ± 0.3^{b}
30Gly10AR	30.5 ± 0.9^{b}	14.8 ± 0.5^{ab}
30Gly20AR	29.0 ± 1.9^{b}	15.1 ± 0.7^{ab}

[a-c]Two means followed by the same letter in the same section and column are not significantly ($p > 0.05$) different through the Tukey's multiple range test.

Cross-linking and physical interactions can improve the water stability and reduce the swelling capacity of gelatin films (Yu et al., 2023). Therefore, to better understand the interactions shown in FTIR analysis, the water resistance and swelling behaviour of films were measured (Fig. 4). Films showed an initial fast water uptake that slowed down around 6 h, and finally got a plateau. Control samples showed intermediated swelling values since SCMC addition increased swelling values while AR addition decreased them. In this sense, films with 20 wt % AR had the lowest swelling values and films with 20 wt % SCMC had the highest ones. Therefore, stronger interactions in films with AR can be confirmed. These physicochemical interactions provide better reinforcement between components, thereby decreasing the degradation or total soluble matter values ($p > 0.05$) in AR-containing films (Table 1). Regarding SCMC-containing films, a higher content of SCMC led to higher swelling values owing to its hydrophilic character (Rakhmatullayeva et al., 2023). However, films with higher content of SCMC showed lower TSM percentages, indicating that the interactions between gelatin, SCMC and citric acid were stronger than the interactions between gelatin and citric acid. Glycerol content did not influence significantly these properties, but swelling values slightly decreased when glycerol content was 30 wt %. This could be due to the presence of physical interactions between gelatin and glycerol, which slowed down the swelling performance of the films. All films showed mean MC values (Table 1) from 14.5 to 17.3%.

3.1.3. Barrier and optical properties

Packaging films must possess high barrier attributes to satisfy the strict protective standard in food packaging applications. Fruit, vegetable, salads and bakery products are the less restrictive foods in terms of water vapour transmission rate requirements (Trinh et al., 2023) and the

Table 2
WVTR values of SCMC- or AR-containing gelatin films with 20 wt % and 30 wt % glycerol.

Film	WVTR (g/m^2·day)
20Control	1510 ± 96^{b}
20Gly10SCMC	1475 ± 75^{b}
20Gly20SCMC	1647 ± 17^{bc}
20Gly10AR	1472 ± 91^{b}
20Gly20AR	1394±4^{a}
30Control	1588 ± 159^{bc}
30Gly10SCMC	1596 ± 116^{bc}
30Gly20SCMC	1764 ± 28^{c}
30Gly10AR	1624 ± 44^{bc}
30Gly20AR	2009 ± 151^{d}

$^{a\text{-}b}$Two means followed by the same letter are not significantly ($p > 0.05$) different through the Tukey's multiple range test.

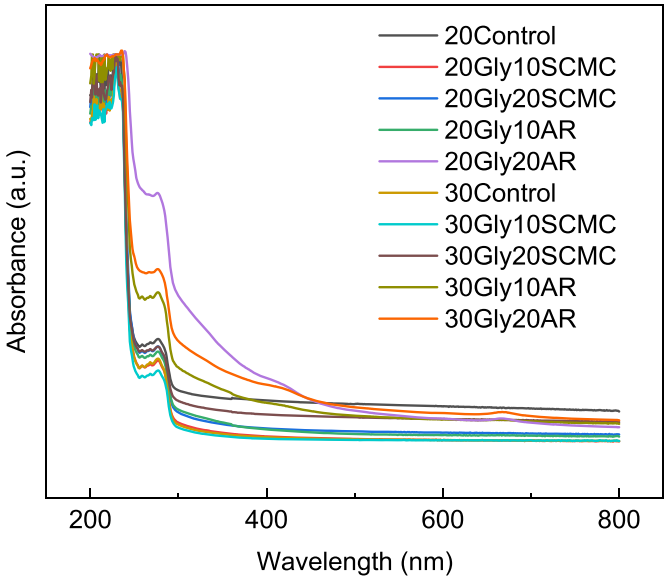

Fig. 5. UV–vis spectra of SCMC- or AR-containing gelatin films with 20 wt % and 30 wt % glycerol.

films prepared in this study fit properly to these requirements. Specifically, films showed WVTR values in the range of 1394–2009 g/m^2·day (Table 2) and in general cellulose did not affect the film WVTR values. As for the plasticizer addition, an increase in glycerol content increased the WVTR values of the films which could be associated with a bigger internal space between polymer chains due to a higher presence of glycerol. Since water vapour transmission is a bulk phenomenon affected not only by surface adsorption but also by the diffusion process through the film, the organization of chains within the film could lead to slight differences, which are not relevant in this work.

Ultraviolet light can harm food quality by producing free radicals able to accelerate food spoilage. In this context, the prepared films owned excellent UV light barrier properties (Fig. 5). Films provided a UV light barrier from 200 to 250 nm, thanks to tyrosine and phenylalanine chromophore aromatic amino acids in gelatin (Lin et al., 2023). UV light absorbance in the 250–280 nm range was influenced by uncrosslinked citric acid, SCMC or AR owing to the carboxyl (chromophore) and hydroxyl (auxochrome) groups present in these substances (Xiang et al., 2022). In this range, control films did not show lowest absorbance values due to the uncrosslinked citric acid. Moreover, by increasing the cellulose content, higher UV light absorbance values were achieved, for instance, 30Gly20AR showed higher absorbance than 30Gly10AR. In summary, films had broad-spectrum UV-resistant activity, providing

Table 3
Colour and gloss values of SCMC- or AR-containing gelatin films with 20 wt % and 30 wt % glycerol.

Film	L*	a*	b*	ΔE*	Gloss (GU)
20Control	96.70 ± 0.49^{a}	−0.20 ± 0.03^{a}	3.39 ± 0.04^{a}	–	15.6 ± 2.7^{b}
20Gly10SCMC	96.41 ± 0.67^{a}	−0.12 ± 0.03^{a}	2.71 ± 0.03^{a}	0.91 ± 0.33^{a}	31.0 ± 5.8^{c}
20Gly20SCMC	96.44 ± 0.09^{a}	−0.18 ± 0.04^{a}	3.13 ± 0.08^{a}	0.39 ± 0.04^{a}	49.1 ± 7.9^{d}
20Gly10AR	87.98 ± 0.95^{c}	−1.37 ± 0.10^{c}	17.52 ± 1.39^{c}	16.66 ± 1.69^{c}	10.9 ± 0.6^{ab}
20Gly20AR	90.68 ± 0.68^{b}	−1.06 ± 0.03^{b}	14.14 ± 0.96^{b}	12.36 ± 1.17^{b}	6.4 ± 0.1^{a}
30Control	96.47 ± 0.40^{a}	−0.14 ± 0.04^{a}	2.89 ± 0.14^{a}	–	17.5 ± 4.2^{b}
30Gly10SCMC	96.75 ± 0.26^{a}	−0.32 ± 0.06^{b}	3.51 ± 0.22^{a}	0.76 ± 0.13^{a}	21.2 ± 2.6^{ab}
30Gly20SCMC	96.47 ± 0.31^{a}	−0.39 ± 0.05^{b}	3.81 ± 0.17^{a}	0.99 ± 0.20^{a}	25.6 ± 4.8^{a}
30Gly10AR	85.16 ± 2.57^{b}	−1.09 ± 0.12^{c}	20.71 ± 2.34^{b}	21.15 ± 3.33^{b}	9.8 ± 1.3^{c}
30Gly20AR	85.42 ± 1.35^{b}	−1.09 ± 0.08^{c}	20.77 ± 1.47^{b}	21.04 ± 1.94^{b}	8.8 ± 0.7^{c}

$^{a\text{-}c}$Two means followed by the same letter in the same section and column are not significantly ($p > 0.05$) different through the Tukey's multiple range test.

films with a secondary antioxidant function (Etxabide et al., 2022).

Concerning colour, L*, a*, b* and ΔE* values were determined (Table 3). As can be seen, the CIELab colour parameters of the films prepared with 20 wt % glycerol were similar ($p > 0.05$) for SCMC-containing films but different ($p < 0.05$) for AR-containing films, AR addition and content varying considerably the colour of the films. Although a* changed with SCMC incorporation, the total colour difference (AE*) in the films prepared with 30 wt % glycerol and SCMC was lower than 1, indicating that there was no visual colour difference. In turn, films prepared with 30 wt % glycerol and AR showed a significant colour change ($p < 0.05$) regardless of AR content. In general, it can be said that SCMC did not change significantly the colour of the films whereas AR did, owing to this residue colour. However, a higher AR content did not suppose a higher colour change, probably due to AR-gelatin interactions, as suggested by swelling results, leading to a more hidden residue. In this sense, a higher content of glycerol (30 wt %) increased the internal space between polymer chains, impliying less hidden residue and increasing colour change.

In terms of gloss, high gloss values are directly correlated with smooth surfaces due to the high degree of random reflection of light in materials with a high degree of roughness. Since gloss values higher than 70, measured at an incidence angle of 60°, indicate glossy and smooth surfaces (Etxabide et al., 2023), film gloss values (<50) were indicative of rough surfaces (Table 3), as observed by SEM images. This roughness was affected by cellulose addition and content, with SCMC leading to smoother surfaces and AR to rougher surfaces. Overall, films prepared with 30 wt % glycerol showed similar or lower gloss values, compared with 20 wt % glycerol-containing films. Even if a lower fibre content was observed on the surface of those films prepared with 30 wt % glycerol, as shown by SEM images, this glycerol content promoted interactions, as found by swelling tests, involving the rearrangement of protein chains and causing the formation of rougher surfaces.

3.1.4. *Thermal properties*

The effect of film composition on thermal properties was studied using DSC analysis (Fig. 6). Films showed an endothermic peak at about 84–117 °C, associated to the energy required for the evaporation of water from the structure (Ahmady et al., 2022). Films prepared with SCMC or AR showed higher evaporation temperatures compared with control films and this behaviour would confirm the interactions between

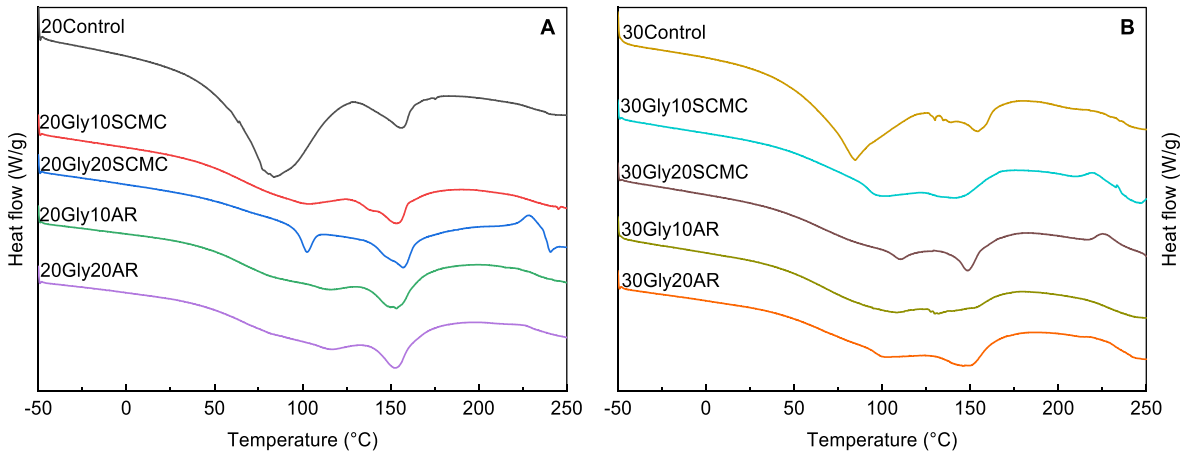

Fig. 6. DSC thermograms of SCMC- or AR-containing gelatin films with (A) 20 wt % and (B) 30 wt % glycerol.

Table 4
Mechanical properties of SCMC- or AR-containing gelatin films with 20 wt % or 30 wt % glycerol.

Film	EM (MPa)	TS (MPa)	EB (%)
20Control	708 ± 60^{a}	21±2^{a}	12±1^{a}
20Gly10SCMC	848 ± 52^{b}	25±2^{b}	13±1^{a}
20Gly20SCMC	901 ± 27^{b}	27±1^{b}	15±1^{b}
20Gly10AR	684 ± 70^{a}	20±2^{a}	10±1^{a}
20Gly20AR	700 ± 61^{a}	22±1^{a}	9±1^{a}
30Control	297 ± 66^{c}	10±1^{c}	19±4^{c}
30Gly10SCMC	327 ± 58^{d}	12±2^{d}	21±2^{c}
30Gly20SCMC	413 ± 13^{d}	15±0^{d}	23±2^{d}
30Gly10AR	440 ± 78^{d}	11±1^{d}	17±1^{c}
30Gly20AR	324±6^{d}	13±2^{d}	17±3^{c}

$^{a\text{-}d}$Two means followed by the same letter in the same column are not significantly ($p > 0.05$) different through the Tukey's multiple range test.

the film components. The second stage, located in the range of 130–160 °C, was associated with the initial thermal decomposition of biopolymers (Deng et al., 2018). The complete thermal decomposition of gelatin consists of the protein chain rupture and the peptide bond breakage (Liu et al., 2023). Besides, the cellulose molecules absorb heat to cleave the glycosidic linkages and other C–C bonds present in glucose, the monomeric backbone of cellulose (Harini & Chandra Mohan, 2020).

3.1.5. *Mechanical properties*

The mechanical response of the films changed depending on the cellulose source present in the film forming formulation (Table 4). The mechanical performance of the films prepared with SCMC was better than that observed for control films, since the increase of SCMC content resulted in the increase of elastic modulus (EM), tensile strength (TS) and elongation at break (EB) values. SCMC was incorporated in the film forming formulation to enhance the mechanical properties of gelatin films by the involvement of hydrogen bonding (Hamdan et al., 2021). However, the addition of AR did not affect the mechanical properties of the films. Comparing films prepared with different glycerol contents,

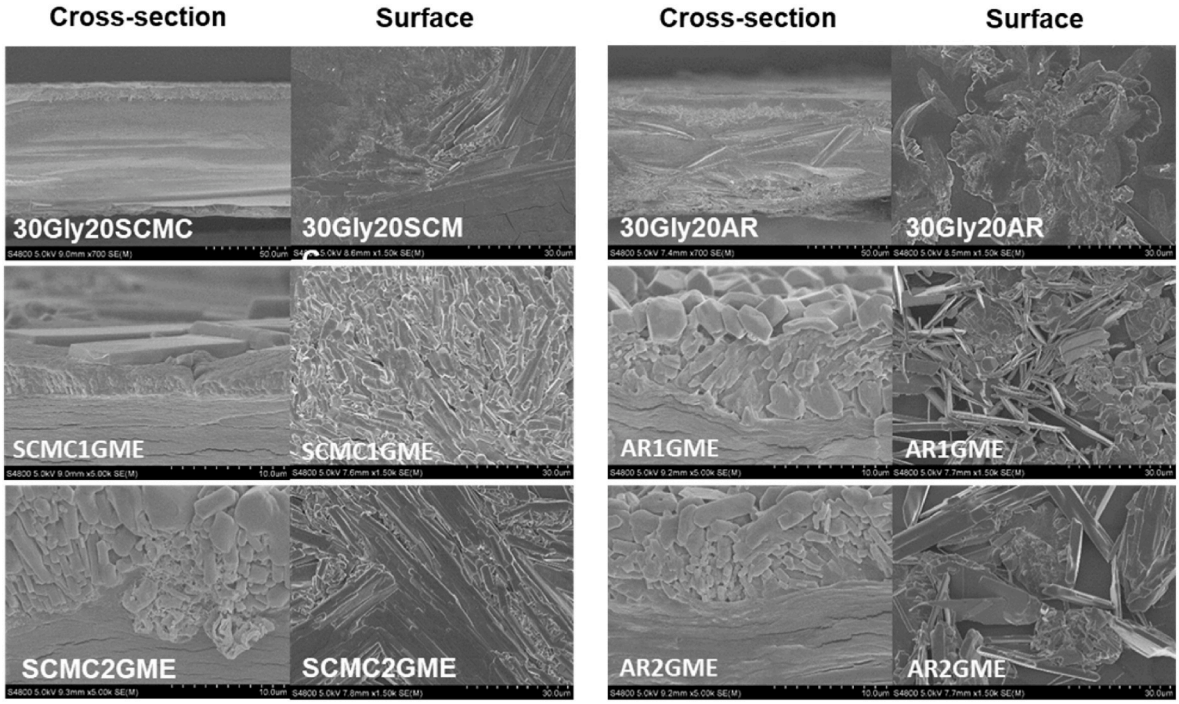

Fig. 7. Cross-sectional and surface SEM images of the films with GME.

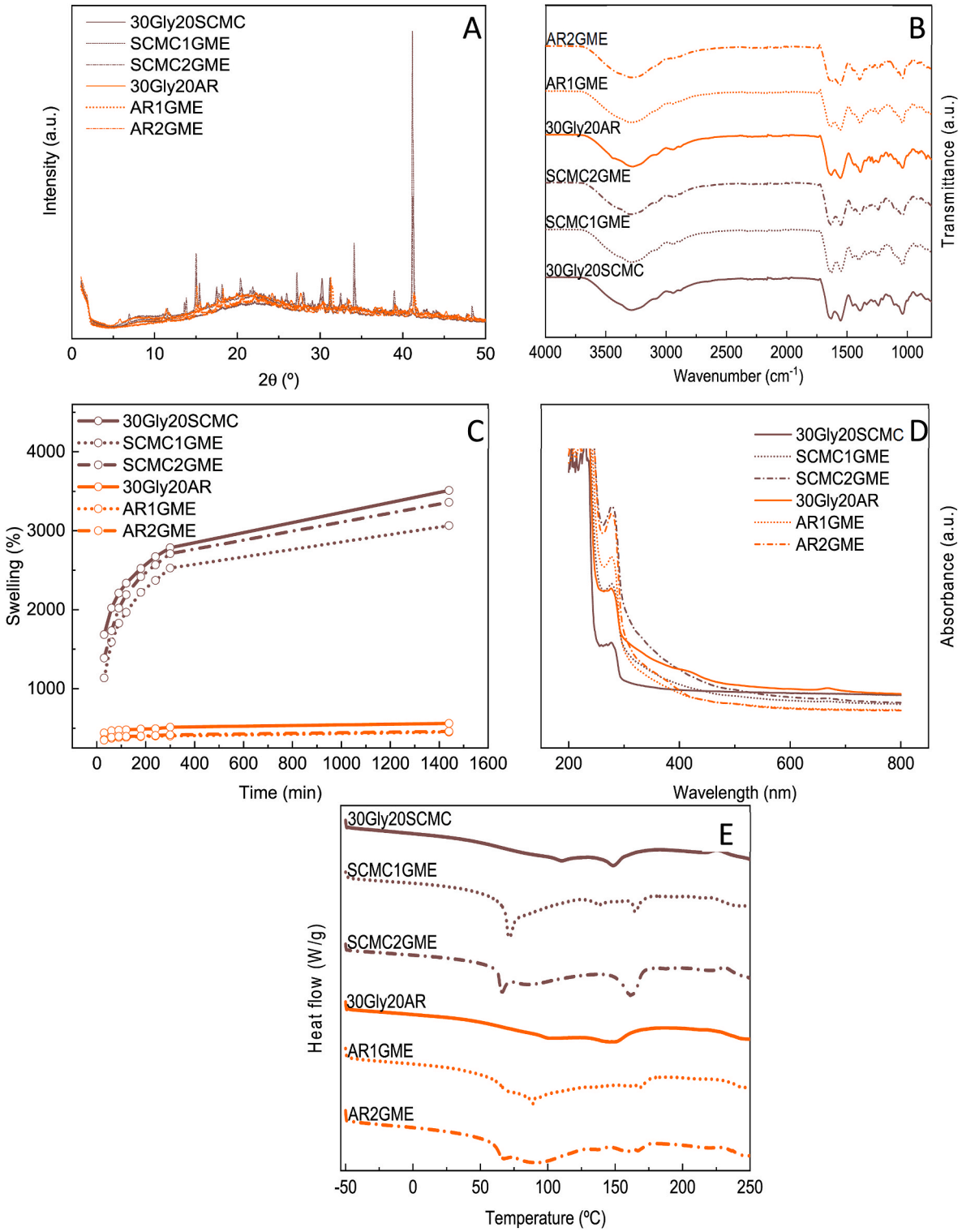

Fig. 8. A) XRD patterns, B) FTIR spectra, C) swelling behaviour, D) UV–vis spectra, and E) DSC thermograms of 30Gly20SCMC and 30Gly20AR gelatin films as a function of GME content.

those with 20 wt % glycerol showed higher EM and TS, but lower EB values.

All in all, films prepared with 30 wt % glycerol and 20 wt % cellulose showed the most appropriate mechanical and UV-light barrier properties and, thus, 30Gly20SCMC and 30Gly20AR films were selected to further analyse the effect of GME addition.

3.2. Characterization of films with GME

3.2.1. GME addition into SCMC/AR-containing films

The pH sensitivity of GME is shown in the Supplementary Data (Fig. S2 ans **S3**). GME-added films were analysed and 30Gly20SCMC and 30Gly20AR were used as control films. As can be seen in Fig. 7, GME addition induced some changes in morphological properties. Films

Table 5
Moisture content (MC), total soluble matter (TSM) and water vapour transmission rate (WVTR) values of 30Gly20SCMC and 30Gly20AR gelatin films as a function of GME content.

Film	MC (%)	TSM (%)	WVTR (g/m^2 day)
30Gly20SCMC	14.5 ± 0.3^a	30.2 ± 3.3^a	1764 ± 28^a
SCMC1GME	16.6 ± 0.8^b	31.5 ± 1.2^a	1803 ± 112^a
SCMC2GME	16.7 ± 1.0^b	27.4 ± 4.0^a	1581 ± 52^b
30Gly20AR	15.1 ± 0.7^a	29.0 ± 1.9^a	2009 ± 151^a
AR1GME	15.5 ± 1.4^a	35.8 ± 2.0^b	2200 ± 354^a
AR2GME	16.4 ± 0.5^a	30.3 ± 0.9^a	1596 ± 23^b

$^{a\text{-}b}$Two means followed by the same letter in the same column are not significantly ($p > 0.05$) different through the Tukey's multiple range test.

Table 6
Colour and gloss values of 30Gly20SCMC and 30Gly20AR gelatin films as a function of GME content.

Film	L*	a*	b*	ΔE*	Gloss (GU)
30Gly20SCMC	96.47 ± 0.31^a	−0.39 ± 0.05^a	3.81 ± 0.17^a	0.99 ± 0.20^a	25.6 ± 4.8^{ab}
SCMC1GME	85.41 ± 0.42^b	4.64 ± 0.19^b	20.29 ± 0.37^b	21.16 ± 0.55^b	22.2 ± 4.1^a
SCMC2GME	85.47 ± 1.40^b	4.10 ± 0.66^b	21.25 ± 1.74^b	21.82 ± 2.29^b	30.1 ± 3.9^b
30Gly20AR	85.42 ± 1.35^a	−1.09 ± 0.08^a	20.77 ± 1.47^a	21.04 ± 1.94^a	8.8 ± 0.7^a
AR1GME	77.59 ± 0.36^b	3.73 ± 0.26^b	24.49 ± 0.41^b	28.95 ± 0.47^b	4.8 ± 0.1^c
AR2GME	74.79 ± 1.80^c	4.57 ± 0.58^c	26.72 ± 1.06^c	32.56 ± 2.05^c	5.7 ± 0.3^b

$^{a\text{-}c}$Two means followed by the same letter in the same section and column are not significantly ($p > 0.05$) different through the Tukey's multiple range test.

prepared with GME showed compact cross-sections, with some agglomerations when GME was incorporated, as also observed in the surface SEM images, where SCMC-containing films show more fibrous-like structures, whereas AR-containing films exhibit dispersed fibres. Considering that films with 30 wt % glycerol displayed space for better orientation of fibres, it could be concluded that GME occupies this space and hinders the oriented fibrous structure of cellulose, leading to visible non-arranged fibres structure.

X-ray diffractograms of pure GME display the typical pattern of semi-crystalline materials with an amorphous broad hump and crystalline peaks. Specifically, GME presents two well-defined crystalline peaks at around 15° and 21° (Coelho et al., 2020; Wang et al., 2019). Therefore, as can be seen in Fig. 8A, when GME content was increased in films, a sharper peak was found around 15°. Additionally, films with GME had other distinguished peaks at 31° and 41° due to the presence of citric acid. Such differences in the crystallinity among the samples could cause differences in film properties and antioxidant activity.

As can be seen in the FTIR spectra (Fig. 8B), the addition of GME did not promote significant changes in gelatin-based film spectra. However, the relative intensity between the amide I and amide II bands changed slightly and this change was even more noticeable in the films prepared with SCMC. This suggested the promotion of interactions due to GME incorporation. Swelling characterization (Fig. 8C) confirmed this result and demonstrated that gelatin films with GME swelled fewest. However, SCMC2GME films showed higher swelling capacity than SCMC1GME films due to the fact that GME is an excellent source of bioactive polyphenols that may have a hydrophilic nature (Ferreira et al., 2014). In this sense, as can be seen in Table 5, MC values of SCMC1GME and SCMC2GME films were higher than those of control films, but all the values are in the range of 15.5–16.7%. Regarding TSM values (Table 5), values were close to 30%, suggesting the dissolution of the glycerol employed in the formulations. Finally, the films with 2 wt % GME showed the lowest WVTR values (Table 5), with all films fitting the

Table 7
Tensile strength (TS) and elongation at bresk (EB) of 30Gly20SCMC and 30Gly20AR gelatin films as a function of GME content.

Film	EM (MPa)	TS (MPa)	EB (%)
30Gly20SCMC	413 ± 13^b	15±0^a	23±2^b
SCMC1GME	459 ± 15^a	23±1^b	38±2^d
SCMC2GME	481 ± 16^a	33±3^c	23±3^b
30Gly20AR	324±6^c	13±2^a	17±3^a
AR1GME	355±9^d	16±1^a	36±0^{cd}
AR2GME	390 ± 11^b	22±2^b	33±2^c

$^{a\text{-}d}$Two means followed by the same letter in the same column are not significantly ($p > 0.05$) different through the Tukey's multiple range test.

WVTR requirements for fruits. These results could be related to the composition of GME, rich in phenolic compounds, whose structure hinders the diffusion of water vapour through the film.

Many studies in the literature have reported that GME has a maximum UV absorption at around 280 nm, indicative of the presence of phenolic compounds (Mugnaini et al., 2024). In this regard, films with GME provided a better UV light barrier between 250 and 300 nm (Fig. 8D), with SCMC2GME and AR2GME films exhibiting similar absorbance values. It is worth highlighting that films remained transparent even at the highest GME concentrations. However, the appearance of control and GME-containing films was different owing to the colour that films acquired when GME was added (Table 6). Results obtained from colour assessment demonstrated that GME-containing films were darker, redder and yellower. The character of non-glossy and rough surfaces was maintained (Table 6). However, the addition of 2 wt % GME increased gloss values, indicating smoother surfaces.

As shown in Fig. 8E, the addition of GME caused changes in the thermal behaviour of films. In films prepared with AR, the addition of GME decreased the temperature of the first endothermic peak, while this temperature increased for the films prepared with SCMC. This increase suggests the promotion of the interactions between GME and the components of the film forming formulations. Moreover, a new peak appeared around 70 °C in films prepared with GME, which may be related to the evaporation of free GME-absorbed moisture (Lu & Hsieh, 2012). On the other hand, the addition of GME may have hindered the degradation of the films, since an increase of the second endothermic peak occurred in relation to that for control films. In addition to the improvement of thermal stability, films with GME showed enhanced mechanical properties since EM ($p < 0.05$), TS ($p < 0.05$) and EB ($p < 0.05$) increased (Table 7). These results can be related to the composition of GME, rich in anthocyanis, phenolic compounds that are known to increase elastic modulus and tensile strength values due to the presence of aromatic ring in their structure; furthermore, their interactions with the polymeric chains by hydrogen bonding also enhance the elongation at break.

3.2.2. GME release and antioxidant activity of films

One of the main benefits of the antioxidant release from packaging materials, compared to the direct addition of antioxidants to food, is that antioxidants can be released in a sustained way (Gómez-Estaca et al., 2014). Thus, the information related to GME release was obtained considering the calibration curve of GME and the absorbance values at specific times. Results showed that the antioxidant release proceeded rapidly throughout the first day, with films (2 cm^2) of SCMC1GME, AR1GME and AR2GME exhibiting a GME release of around 50% after 24 h; in the case of SCMC2GME films, the release was 72%. Then, the release continued and, at the end of the second day, different release percentages were observed, in particular, 76, 87, 55 and 64% for SCMC1GME, SCMC2GME, AR1GME and AR2GME, respectively. AR-containing films formed networks that hinder the release of the extract even more than films with SCMC. Therefore, depending on the end application, their suitability should be different.

Malvidin-3-O-glucoside and catechin are prominent representative

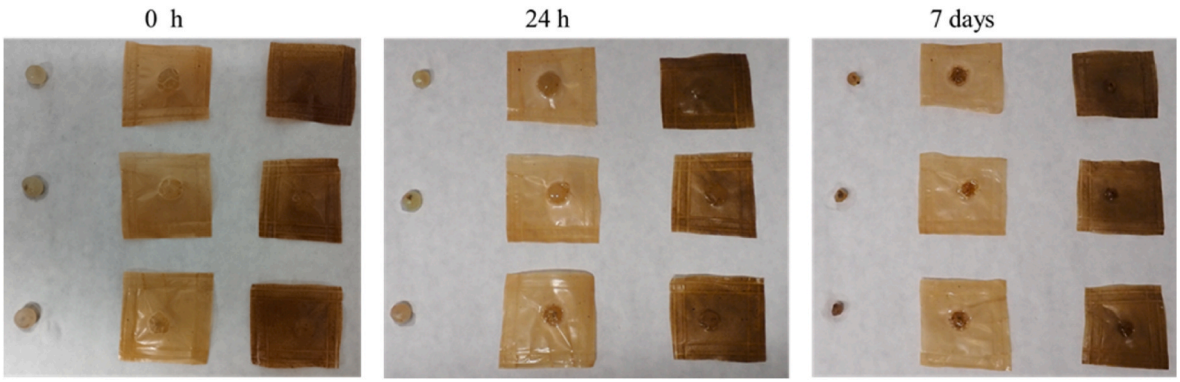

Fig. 9. Preservation study of grapes (0 h, 24 h and 7 days). In each image, from left to right: grape without packaging, grape packaged in SCMC2GME films, and grape packaged in AR2GME films.

Table 8
Changes in grapes after packaging: colour, pH and Brix percentage.

Film	Colour change	pH increase	Brix % increase
No packaging	20±4[a]	1.6 ± 0.2[a]	64±3[a]
SCMC2GME	16±4[b]	1.7 ± 0.6[a]	59±2[a]
AR2GME	20±4[a]	2.9 ± 0.4[b]	57±4[a]

[a-b]Two means followed by the same letter in the same section and column are not significantly ($p > 0.05$) different through the Tukey's multiple range test.

compounds of anthocyanins and flavan-3-ols, respectively. Based on a previous study (Vandermeer, 2020), both phenolic compounds are present in the grape marc extract employed. These phenolic compounds within the extract have a direct impact on its free radical scavenging ability. Indeed, SCMC1GME, SCMC2GME, AR1GME and AR2GME 1 cm^2 films showed 11, 41, 14 and 30% inhibition at 48 h, promising results that highlight the potential of these films for active packaging.

3.2.3. *Application of films in the conservation of peeled grapes*

Sulfur dioxide treatment is a widespread and effective method to prevent grapes rot, but the residues of sulfites in grapes raise consumer health are a concerning issue (Gong et al., 2023). This way, gentle handling, careful cluster cleaning, low storage temperature, dipping in ethanol prior to packaging and compounds alternative to sulfur dioxide are proposed to reduce the incidence of grape degradation (Costa et al., 2011). Even if different strategies were investigated for table grapes (Zeng et al., 2024; Zhao et al., 2022), to the best of our knowledge no manuscript has been focused on the peeled grape packaging. Since, these peeled grapes are now sold in supermarkets, research on alternative materials is needed and, thus, films prepared with grape marc extract were employed for peeled grapes packaging, closing the loop. Since the appearance change is the most intuitive way for quality evaluation, this changes in grapes during storage were observed and photographed (Fig. 9). On the 7th day of storage, the browning of peeled grapes occurred and a slight shrinkage was observed.

Changes were further analysed via colour, pH and Brix assessment of the grapes once out of the packaging (Table 8). Regarding colour change, all grapes showed changes but grapes packaged with SCMC2GME films exhibited the lowest ($p < 0.05$) changes. Apart from colour change, the titratable acidity of all grapes gradually decreased during the whole storage period. The loss of acidity during maturation is due to decarboxylation of tricarboxylates to produce dicarboxylates, followed by decarboxylation to produce phosphoenolpyruvic acid and activate of gluconeogenesis, leading to the degradation of organic acids (Zeng et al., 2024). Grapes packaged with SCMC2GME films exhibited lower pH changes. According to Brix change, although there was no significant change ($p > 0.05$) between packaged and non-packaged grapes, packaged grapes showed lower values and, specifically, the lowest values were recorded for grapes packaged with AR2GME. These results demonstrated that the films developed could benefit grapes packaging.

4. Conclusions

The incorporation of cellulose from different sources and different glycerol contents into gelatin film forming solutions modified the properties of the resulting films, with the films with 30 wt% glycerol and 20 wt % cellulose showing the best performance. Therefore, GME was added into 30Gly20SCMC and 30Gly20AR to analyse their antioxidant capacity and their potential as active packaging films. Films exhibited semi-crystalline character and compact structure, free of cracks and visible pores. Additionally, FTIR findings suggested that interactions were more noticeable in films with AR, rather than in films with SCMC. Furthermore, a promotion of interactions between the components was observed due to the extract incorporation, as corroborated by swelling tests. These interactions led to lower total soluble matter values in cellulose-containing films. Films fitted properly WVTR requirements for fruits and showed excellent UV barrier properties, improved by cellulose and GME addition, which did not interfere with the transparency of the films. Moreover, thermal stability and mechanical properties were enhanced with cellulose and GME incorporation. Regarding antioxidant properties, AR-containing films formed networks that promote the sustained release of the extract even more than the films with SCMC. On top of that, GME-containing films contributed an improvement to peeled grapes packaging. In particular, the films prepared with 2 wt % GME showed the lowest WVTR values with smoother surfaces, enhanced tensile resistance, higher free radical scavenging ability, and grapes packaged with these films exhibited lower pH changes.

CRediT authorship contribution statement

Jone Uranga: Writing – original draft, Investigation, Formal analysis, Data curation. **Itsaso Leceta:** Writing – review & editing, Investigation, Formal analysis, Data curation. **Pedro Guerrero:** Writing – review & editing, Validation, Supervision, Resources, Methodology, Investigation, Funding acquisition, Conceptualization. **Koro de la Caba:** Writing – review & editing, Validation, Supervision, Resources, Project administration, Methodology, Investigation, Funding acquisition, Conceptualization.

Declaration of competing interest

The authors declare that they have no known competing financial interests or personal relationships that could have appeared to influence the work reported in this paper.

Data availability

Data will be made available on request.

Acknowledgments

This work was supported by the Basque Government (IT1658-22 and Elkartek Program). J. Uranga thanks the University of the Basque Country (ESPDOC21/74).

Appendix A. Supplementary data

Supplementary data to this article can be found online at https://doi.org/10.1016/j.foodhyd.2024.109951.

References

Ahmady, A. R., Razmjooee, K., Saber-Samandari, S., & Toghraie, D. (2022). Fabrication of chitosan-gelatin films incorporated with thymol-loaded alginate microparticles for controlled drug delivery, antibacterial activity and wound healing: In-vitro and in-vivo studies. *International Journal of Biological Macromolecules, 223*, 567–582.

Alipal, J., et al. (2021). A review of gelatin: Properties, sources, process, applications, and commercialisation. *Materials Today Proceedings, 42*, 240–250.

Andonegi, M., de la Caba, K., & Guerrero, P. (2020). Effect of citric acid on collagen sheets processed by compression. *Food Hydrocolloids, 100*, Article 105427.

Azarifar, M., Ghanbarzadeh, B., Sowti khiabani, M., Akhondzadeh basti, A., & Abdulkhani, A. (2020). The effects of gelatin-CMC films incorporated with chitin nanofiber and Trachyspermum ammi essential oil on the shelf life characteristics of refrigerated raw beef. *International Journal of Food Microbiology, 318*, Article 108493.

Chen, L., Qiang, T., Chen, X., Ren, W., & Zhang, H. J. (2022). Gelatin from leather waste to tough biodegradable packaging film: One valuable recycling solution for waste gelatin from leather industry. *Waste Management, 145*, 10–19.

Coelho, C. C. de S., et al. (2020). Cellulose nanocrystals from grape pomace and their use for the development of starch-based nanocomposite films. *International Journal of Biological Macromolecules, 159*, 1048–1061.

Commission Regulation (EU) No 10/2011 of 14 January 2011 on plastic materials and articles intended to come into contact with food.

Costa, C., et al. (2011). Effects of passive and active modified atmosphere packaging conditions on ready-to-eat table grape. *Journal of Food Engineering, 102*, 115–121.

Deng, L., et al. (2018). Characterization of gelatin/zein nanofibers by hybrid electrospinning. *Food Hydrocolloids, 75*, 72–80.

Dharmalingam, K., & Anandalakshmi, R. (2019). Fabrication, characterization and drug loading efficiency of citric acid crosslinked NaCMC-HPMC hydrogel films for wound healing drug delivery applications. *International Journal of Biological Macromolecules, 134*, 815–829.

Diop, C. I. K., Beltran, S., Sanz, M.-T., Garcia-Tojal, J., & Trigo-lopez, M. (2023). Designing bilayered composite films by direct agar/chitosan and citric acid-crosslinked PVA/agar layer-by-layer casting for packaging applications. *Food Hydrocolloids, 144*, Article 108987.

Etxabide, A., Arregi, M., Cabezudo, S., Guerrero, P., & de la Caba, K. (2023). Whey protein films for sustainable food packaging: Effect of incorporated ascorbic acid and environmental assessment. *Polymers, 15*, 387.

Etxabide, A., Yang, Y., Maté, J. I., de la Caba, K., & Kilmartin, P. A. (2022). Developing active and intelligent films through the incorporation of grape skin and seed tannin extracts into gelatin. *Food Packaging and Shelf Life, 33*, Article 100896.

Ferreira, A. S., Nunes, C., Castro, A., Ferreira, P., & Coimbra, M. A. (2014). Influence of grape pomace extract incorporation on chitosan films properties. *Carbohydrate Polymers, 113*, 490–499.

Gil-Martín, E., et al. (2022). Influence of the extraction method on the recovery of bioactive phenolic compounds from food industry by-products. *Food Chemistry, 378*, Article 131918.

Gómez-Estaca, J., López-de-Dicastillo, C., Hernández-Muñoz, P., Catalá, R., & Gavara, R. (2014). Advances in antioxidant active food packaging. *Trends in Food Science & Technology, 35*, 42–51.

Gong, D., et al. (2023). Development of Vitamin C/polyurethane composite films for efficient preservation of grapes with controllable respiration. *Lebensmittel-Wissenschaft & Technologie, 184*, Article 115086.

Guo, Y. Z., et al. (2022). Facile preparation of cellulose hydrogel with Achilles tendon-like super strength through aligning hierarchical fibrous structure. *Chemical Engineering Journal, 428*, Article 132040.

Hamdan, M. A., Ramli, N. A., Othman, N. A., Mohd Amin, K. N., & Adam, F. (2021). Characterization and property investigation of microcrystalline cellulose (MCC) and carboxymethyl cellulose (CMC) filler on the carrageenan-based biocomposite film. *Materials Today Proceedings, 42*, 56–62.

Harini, K., & Chandra Mohan, C. (2020). Isolation and characterization of micro and nanocrystalline cellulose fibers from the walnut shell, corncob and sugarcane bagasse. *International Journal of Biological Macromolecules, 163*, 1375–1383.

Hassan, M. M., Tucker, N., & Le Guen, M. J. (2020). Thermal, mechanical and viscoelastic properties of citric acid-crosslinked starch/cellulose composite foams. *Carbohydrate Polymers, 230*, Article 115675.

Jayasena, V. (2008). & Cameron, I. °brix/Acid ratio as a predictor of consumer acceptability of crimson seedless table grapes. *Journal of Food Quality, 31*, 736–750.

Jelley, R. E., Deed, R. C., Barker, D., Parish-Virtue, K., & Fedrizzi, B. (2020). Fermentation of Sauvignon blanc grape marc extract yields important wine aroma 3-sulfanylhexan-1-ol (3SH). *Lebensmittel-Wissenschaft & Technologie, 131*, Article 109653.

Li, H., Shi, H., He, Y., Fei, X., & Peng, L. (2020). Preparation and characterization of carboxymethyl cellulose-based composite films reinforced by cellulose nanocrystals derived from pea hull waste for food packaging applications. *International Journal of Biological Macromolecules, 164*, 4104–4112.

Lin, B., et al. (2023). Characterization of anglerfish gelatin/polyvinyl alcohol film and its application in preservation of small yellow croaker (Larimichthys polyactis). *Journal of Food Engineering, 357*, Article 111641.

Liu, F., Antoniou, J., Li, Y., Ma, J., & Zhong, F. (2015). Effect of sodium acetate and drying temperature on physicochemical and thermomechanical properties of gelatin films. *Food Hydrocolloids, 45*, 140–149.

Liu, Y., et al. (2023). Effect of catechin and tannins on the structural and functional properties of sodium alginate/gelatin/poly(vinylalcohol) blend films. *Food Hydrocolloids, 135*, Article 108141.

Liu, B., Wang, J., Zhang, Y., Liu, D., & Zhang, Y. (2022). Structure and properties of gelatin edible film modified using oxidized poly(2-hydroxyethyl acrylate) with multiple aldehyde groups. *Journal of the Science of Food and Agriculture, 102*, 6349–6357.

Lu, P., & Hsieh, Y.-L. (2012). Cellulose isolation and core–shell nanostructures of cellulose nanocrystals from chardonnay grape skins. *Carbohydrate Polymers, 87*, 2546–2553.

Ludmerczki, R., et al. (2019). Carbon dots from citric acid and its intermediates formed by thermal decomposition. *Chemistry - A European Journal, 25*, 11963–11974.

Luo, Q., et al. (2022). Gelatin-based composite films and their application in food packaging: A review. *Journal of Food Engineering, 313*, Article 110762.

Mondal, M. I. H., Yeasmin, M. S., & Rahman, M. S. (2015). Preparation of food grade carboxymethyl cellulose from corn husk agrowaste. *International Journal of Biological Macromolecules, 79*, 144–150.

Mugnaini, G., et al. (2024). Effect of design and molecular interactions on the food preserving properties of alginate/pullulan edible films loaded with grape pomace extract. *Journal of Food Engineering, 361*, Article 111716.

Nguyen, Q.-D., Tran, T. T. V., Nguyen, N.-N., Nguyen, T.-P., & Lien, T.-N. (2023). Preparation of gelatin/carboxymethyl cellulose/guar gum edible films enriched with methanolic extracts from shallot wastes and its application in the microbiological control of raw beef. *Food Packaging and Shelf Life, 37*, Article 101091.

Rachtanapun, P., Luangkamin, S., Tanprasert, K., & Suriyatem, R. (2012). Carboxymethyl cellulose film from durian rind. *LWT-Food Science & Technology, 48*, 52–58.

Rakhmatullayeva, D., et al. (2023). Development and characterization of antibacterial coatings on surgical sutures based on sodium carboxymethyl cellulose/chitosan/chlorhexidine. *International Journal of Biological Macromolecules, 236*, Article 124024.

Salimiraad, S., Safaeian, S., Basti, A. A., Khanjari, A., & Nadoushan, R. M. (2022). Characterization of novel probiotic nanocomposite films based on nano chitosan/nano cellulose/gelatin for the preservation of fresh chicken fillets. *Lebensmittel-Wissenschaft & Technologie, 162*, Article 113429.

Samsi, M. S., Kamari, A., Din, S. M., & Lazar, G. (2019). Synthesis, characterization and application of gelatin–carboxymethyl cellulose blend films for preservation of cherry tomatoes and grapes. *Journal of Food Science & Technology, 56*, 3099–3108.

Shi, R., et al. (2007). Characterization of citric acid/glycerol co-plasticized thermoplastic starch prepared by melt blending. *Carbohydrate Polymers, 69*, 748–755.

Toniciolli Rigueto, C. V., et al. (2022). Gelatin films from wastes: A review of production, characterization, and application trends in food preservation and agriculture. *Food Research International, 162*, Article 112114.

Trinh, B. M., Chang, B. P., & Mekonnen, T. H. (2023). The barrier properties of sustainable multiphase and multicomponent packaging materials: A review. *Progress in Materials Science, 133*, Article 101071.

Uranga, J., Carranza, T., Peñalba, M., de la Caba, K., & Guerrero, P. (2023). Valorization of agar production residue as a filler in soy protein hydrogels for 3D printing. *Int. J. Bioprinting, 9*, 731.

Uranga, J., Leceta, I., Etxabide, A., Guerrero, P., & de la Caba, K. (2016). Cross-linking of fish gelatins to develop sustainable films with enhanced properties. *European Polymer Journal, 78*, 82–90.

Usman, M., Ishaq, A., Regenstein, J. M., Sahar, A., Aadil, R. M., Sameen, A., Khan, M. I., & Alam, A. (2023). *Valorization of animal by-products for gelatin extraction using conventional and green technologies: A comprehensive review*. Biomass Conversion and Biorefinery. https://doi.org/10.1007/s13399-023-04547-5

Vandermeer, C. J. Promising natural extracts for use in active food packaging.

Vargas-Torrico, M. F., von Borries-Medrano, E., & Aguilar-Méndez, M. A. (2022). Development of gelatin/carboxymethylcellulose active films containing Hass avocado peel extract and their application as a packaging for the preservation of berries. *International Journal of Biological Macromolecules, 206*, 1012–1025.

Wang, S., Gu, B.-J., & Ganjyal, G. M. (2019). Impacts of the inclusion of various fruit pomace types on the expansion of corn starch extrudates. *Lebensmittel-Wissenschaft & Technologie, 110*, 223–230.

Wang, Y., Zhang, J., & Zhang, L. (2022). An active and pH-responsive film developed by sodium carboxymethyl cellulose/polyvinyl alcohol doped with rose anthocyanin extracts. *Food Chemistry, 373*, Article 131367.

Xiang, H., et al. (2022). Enzymatically synthesized γ-[Glu](n≥1)-Gln as novel calcium-binding peptides to deliver calcium with enhanced bioavailability. *Food Chemistry, 387*, Article 132918.

Xiao, Q., Gu, X., & Tan, S. (2014). Drying process of sodium alginate films studied by two-dimensional correlation ATR-FTIR spectroscopy. *Food Chemistry, 164*, 179–184.
Yu, H., Ge, Y., Ding, H., Yan, Y., & Wang, L. (2023). Vanillin cross-linked chitosan/gelatin bio-polymer film with antioxidant, water resistance and ultraviolet-proof properties. *International Journal of Biological Macromolecules, 253*, Article 126726.
Zeng, Y.-F., et al. (2024). Preparation and characterization of lotus root starch based bioactive edible film containing quercetin-encapsulated nanoparticle and its effect on grape preservation. *Carbohydrate Polymers, 323*, Article 121389.
Zhang, W., Roy, S., Assadpour, E., Cong, X., & Jafari, S. M. (2023). Cross-linked biopolymeric films by citric acid for food packaging and preservation. *Advances in Colloid and Interface Science, 314*, Article 102886.
Zhao, X., Tian, R., Zhou, J., & Liu, Y. (2022). Multifunctional chitosan/grape seed extract/silver nanoparticle composite for food packaging application. *International Journal of Biological Macromolecules, 207*, 152–160.
Zujovic, Z., Ray, S., Vandermeer, C., Bowmaker, G. A., & Kilmartin, P. (2021). Influnece of grape marc extract on tuning the intermolecular interaction in the high-density polyethylene. *Journal of Applied Polymer Science, 138*, Article 50605.